UNITECH SELECTED PAPERS

International Scientific Conference
UNITECH`2024

MOLECULAR DYNAMICS SIMULATION STUDY OF STATIC AND DYNAMIC PROPERTIES OF LIQUID Fe UNDER HIGH PRESSURE

Cem Canan[1], Murat Celtek[2], Unal Domekeli[3]

[1]*Edirne Vocational College of Technical Science, Trakya University, 22030, Edirne – Türkiye*
[2]*Faculty of Education, Trakya University, 22030, Edirne – Türkiye*
[3]*Dept. of Physics, Trakya University, 22030, Edirne – Türkiye*

** Corresponding author: cemcanan@trakya.edu.tr*

Abstract

As is known, the core of our Earth is largely composed of iron (Fe). This core consists of an inner solid Fe core and an outer liquid Fe core under high temperature and pressure. It is very difficult to experimentally determine the physical properties of liquid Fe under these thermodynamic conditions. Therefore, atomic simulations are a good alternative to understand the behavior of the liquid core. In this study, we investigated the static and dynamic properties of liquid Fe under high pressure and high temperature using the classical molecular dynamics (MD) simulation method. In MD simulations, many-body tight-binding (TB) potentials were used to describe the interatomic interactions. Liquid Fe at 3000 K above the melting point was simulated under ten different thermodynamic conditions starting from ambient pressure to 90 GPa. Static and dynamic properties such as density, pair distribution function, self-diffusion coefficient and shear-viscosity were analyzed depending on the pressure. The results obtained from the MD simulation are in good agreement with the available experimental results.

Keywords: MD simulations, liquid Fe, high pressure, many-body tight-binding potentials.

INTRODUCTION

The Earth's core is predominantly composed of Fe, which exists in two different phases: the solid inner core and the liquid outer core. Understanding the structure, dynamics, and the geophysical phenomena driven by these dynamics, such as the generation of the Earth's magnetic field and heat and mass transport, is crucial for studying fundamental processes. A detailed examination of the properties of liquid Fe under high pressure and temperature conditions is essential for modeling these processes. However, direct experimental measurements under such extreme conditions are extremely challenging. On the other hand, experimental studies have also significantly contributed to understanding the thermodynamic and structural properties of iron [1–7]. For example, Inui et al. [8] used x-ray diffraction (XD) and Schenk et al. [9] neutron diffraction method to determine the static structure factor (SF) of liquid Fe close to its melting point at 0 GPa. Shen et al. [10] extended XD measurements of SF to pressures up to 58 GPa, and Kuwayama et al. [11] reached 116 GPa. Across this range, SF retains a shape similar to that observed at 0 GPa. Theoretical studies and computational approaches such as classical MD (CMD), ab-initio (AIMD) simulations, which are frequently used on the structure and dynamic properties of liquid Fe under high pressure and temperature, have provided important information on the thermodynamic, structural and electronic properties of liquid Fe [12,13]. CMD simulations have been explored the entire pressure range from ambient conditions to the liquid phases, using mainly the embedded-atom model by Sutton & Chen [14], Belonoshko et al. [15]. This model has been widely applied to study static structure and transport properties of liquid Fe at various conditions [16–18]. In contrast, AIMD simulations have primarily focused on the high-pressure, high-temperature

doi: www.doi.org/10.70456/.....

regimes. First, Vocadlo et al. [19] studied the SF of liquid Fe at 4300–6000 K, and subsequent studies investigated the structural and dynamic properties, adiabatic sound speed, and pressure-temperature phase diagram of liquid Fe under relevant conditions [13,20,21]. In this study, we used CMD simulations with many-body TB potentials to study the static and dynamic properties of liquid Fe under high pressure and temperature. Above its melting point, liquid Fe at 3000 K was analyzed under different pressures ranging from ambient pressure to 90 GPa, focusing on density, pair distribution function (PDF), self-diffusion coefficient and shear-viscosity.

EXPOSITION

In this study, we used the many-body TB potential to describe the interactions between liquid Fe atoms in CMD simulations. According to the many-body TB potential, the total energy, E^i_c, as the sum of the attractive and repulsive terms is written as [22]:

$$E_c^i = \sum_i (E_R^i + E_B^i) \tag{1}$$

where E^i_R and E^i_B are the repulsive and attractive terms of the total energy, respectively, and are given as:

$$E_R^i = \sum_j A\, exp\left[-p\left(\frac{r_{ij}}{r_o}-1\right)\right] \tag{2}$$

$$E_B^i = -\left\{\sum_j \xi^2\, exp\left[-2q\left(\frac{r_{ij}}{r_o}-1\right)\right]\right\}^{1/2} \tag{3}$$

were, r_{ij} represents the distance between atoms i and j, and r_o denotes the nearest-neighbor distance. A, ξ, p, and q are model parameters related to the elements physical properties. The many-body TB potential parameters for Fe are listed in Table 1 [23].

Table. 1. *TB potential parameters for Fe* [23].

A(eV)	*ξ(eV)*	*p*	*q*	*r_0(Å)*
0.1184	*1.5818*	*10.7613*	*2.0378*	*2.4824*

We performed all CMD simulations for liquid Fe using the parallel code DLPOLY simulation package [24]. Initially, the liquid Fe model was created by randomly distributing 8192 atoms in a cubic box and periodic boundary conditions were applied to this model in three directions. Then, the model system was equilibrated using 200000 MD steps with the isothermal isobaric (NPT) canonical ensemble under the desired thermodynamic conditions. The equilibrated model system was simulated using the NPT ensemble with 100000 MD steps at T=1830 K and 0 GPa, and at T=3000 K and 0, 10, 20, 30, 40, 50, 60, 70, 80 and 90 GPa, respectively. The first 50000 MD time steps of the 100000 MD time steps were used to equilibrate the system at the desired thermodynamic state, while the last 50000 MD time steps were used to generate time-averaged features. The classical equations of motion are integrated using the Leapfrog-Verlet algorithm with a time step of 1fs. The temperature and pressure of the system are controlled by the Nose-Hoover thermostat and the Berendsen borastat, respectively.

The atomistic structure in liquids is usually characterized by the PDF and the static SF, which is the Fourier transform of the PDF. Since the calculations in MD simulations are performed in real space, the liquid structure was analyzed using the pair distribution function. The expression of the PDF, $g(r)$, is given as [25]:

$$g(r) = \frac{\Omega}{N^2}\left\langle \sum_i^N \sum_{i\neq j}^N \delta(r - r_{ij}) \right\rangle \tag{4}$$

where N and Ω represent the number of atoms, and volume of the simulations cell, respectively. The PDF obtained from the MD simulation for liquid Fe at 0 GPa at T=1830 K is plotted in comparison with the experimental result from Waseda [26] in Figure 1. As seen from Figure 1, the peak positions and amplitudes of the PDF obtained from the MD simulation are in good agreement with the experimental result. This result is a clear indication that

the many-body TB potential used in the MD simulations accurately describes the Fe-Fe interactions in the liquid phase.

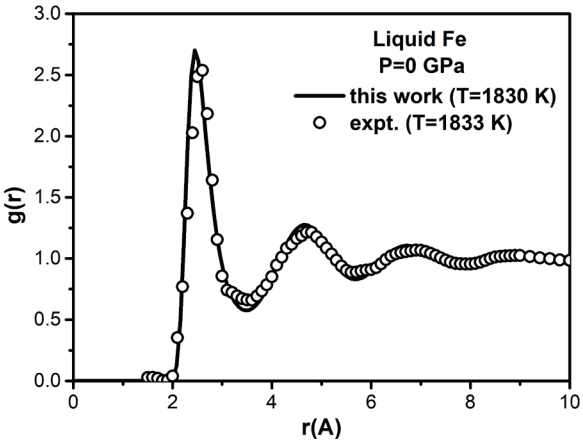

Fig. 1. *PDFs of liquid Fe simulated under 0 GPa at 1830 K (experimental result under 0 GPa at 1833 K).*

To investigate the effect of high pressure on the atomistic structure of liquid Fe at 3000 K, the sample was simulated under different pressure values from ambient pressure to 90 GPa. The PDFs of liquid Fe under different pressures at 3000 K are given in Figure 2.

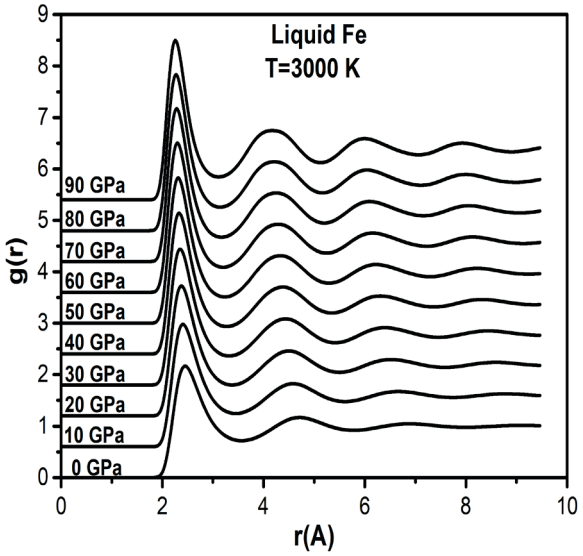

Fig. 2. *PDFs of liquid Fe under different pressures at 3000 K.*

The PDFs obtained under each pressure converge smoothly at large *r* values. This means that the atoms in the liquid system are randomly distributed. As expected, the positions of the first, second, third and fourth peaks of the PDF move towards small r values with increasing pressure; on the other hand, the peak amplitudes increase. For example, the amplitude of the main peak increases from 2.16 at ambient pressure to 3.12 at P=90 GPa. The variations in the positions of the first, second, third and fourth peaks of the PDF as a function of pressure are plotted in Figure 3.

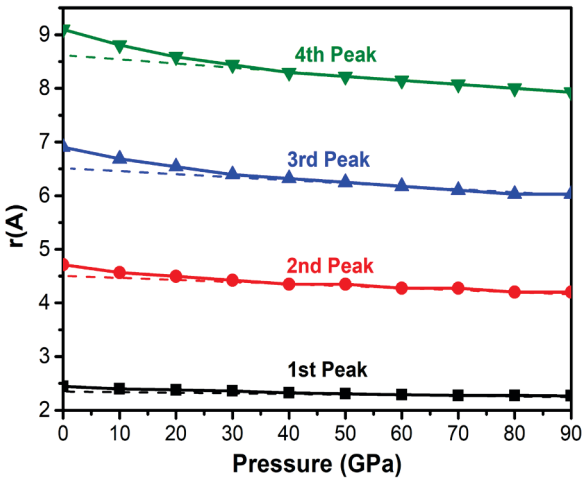

Fig. 3. *First, second, third and fourth peak positions of PDF of liquid Fe under different pressures at T=3000 K.*

As is known, the position of each peak in the PDF corresponds to the first, second, third and fourth nearest neighbor distances, respectively. These nearest neighbor distances decrease with increasing pressure. The rate of decrease in neighbor distances for each is greater up to 30 GPa, while after 30 GPa the nearest neighbor distances decrease linearly with pressure. However, the amount of decrease in the distance of each nearest neighbor is different from each other. The amount of decrease in the first, second, third and fourth nearest neighbor distances is 7.15%, 10.85%, 12.69% and 12.85%, respectively. These results show that the amount of decrease is at least at the first nearest neighbor distance and at most at the fourth nearest neighbor distance. It can even be said that the pressure effect on the third and fourth nearest neighbors is the same. In Figure 4, the densities obtained from MD simulations under different pressures at 3000 K are compared with the experimental results obtained using *in situ*

XRD technique by Kuwayama et al. [11]. As can be seen from Figure 4, the densities obtained from MD are in excellent agreement with the experimental results at each pressure value. As expected, the density increase as the pressure increases. This increase exhibits a nonlinear behavior with pressure up to approximately 30 GPa, while it exhibits a linear behavior after 30 GPa.

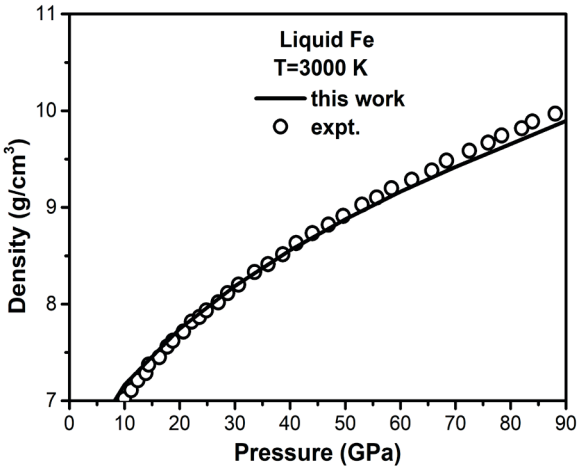

Fig. 4. *Density of liquid Fe as a function of pressure at 3000 K.*

In this study, the dynamic behavior of liquid Fe under high pressure was determined by analyzing physical quantities such as self-diffusion and shear-viscosity. The self-diffusion coefficient, D, is calculated by using the Einstein equation:

$$D = \lim_{t\to\infty} \frac{MSD}{6t} \tag{5}$$

where t is the diffusion time, MSD of the atom in the MD simulations can be described as [27]:

$$MSD = \frac{1}{N}\sum_{i=1}^{N} \left| r_i(t+t_o) - r_i(t_o) \right|^2 \tag{6}$$

where $r_i\,(t_o)$ is the position vector of the ith atom for the system in its initial configuration and $r_i\,(t)$ is the position vector of ith atom at time t. In MD simulations, shear-viscosity can often be estimated using the Stokes-Einstein equation, which relates the self-diffusion coefficient of a macroscopic particle of diameter r to the shear viscosity of the fluid in which the particle is moving [13]. According to this equation, the shear-viscosity, η, is defined as [13]:

$$\eta = \frac{k_B T}{2\pi r D} \tag{7}$$

where k_B, T and D are the Boltzmann constant, temperature and self-diffusion coefficient, respectively. In liquid metals, r is the position of the main peak of the PDF [13]. D and η values obtained from the MD simulations for liquid Fe at 3000K are plotted as a function of pressure in Figure 5.

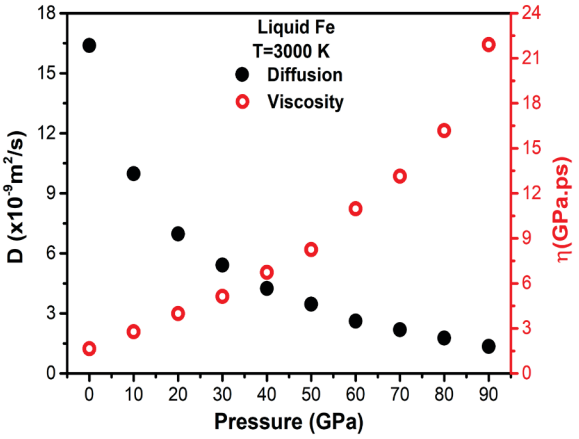

Fig. 5. *The self-diffusion coefficient and shear-viscosity of liquid Fe as a function of pressure at 3000 K.*

With increasing pressure, the self-diffusion coefficient decreases, while the shear-viscosity increases. The rate of change of the self-diffusion coefficient is high up to approximately 30 GPa, but after 30 GPa it decreases almost linearly with pressure. When the pressure is increased from 0 to 90 GPa, the self-diffusion coefficient decreases by approximately 91.7%. On the other hand, shear viscosity increases linearly with pressure up to about 30 GPa, and begins to increase significantly after 30 GPa. When the pressure is increased from 0 to 90 GPa, the shear-viscosity increases by approximately 92.5%. These results show that high pressure suppresses the mobility of liquid Fe atoms and thus causes an increase in shear-viscosity.

CONCLUSION

In this study, we examined the high pressure effect on the static and dynamic properties of liquid Fe using the CMD simulations technique with the many-body TB potential. For this purpose, the simulations were performed out under thermodynamic conditions ranging from ambient pressure to 90 GPa at T=3000K. The PDF and densities obtained from CMD are in very good agreement with the experimental results. These results demonstrate how accurately the many-body TB potentials used in the simulation describe the interatomic interactions for liquid iron. From the pressure-dependent behavior of the static structure, we observed that the positions of the first, second, third and fourth nearest neighbor atoms in the liquid system shift towards smaller *r* values with increasing pressure. This indicates that the atoms in the liquid system become more densely packed with increasing pressure. The third and fourth nearest neighbors are more affected by the pressure effect than the first and second nearest neighbors. In addition, at 3000 K, the static structure is more affected by pressure up to a critical pressure value of 30 GPa, after which the pressure effect weakens with increasing pressure. Similarly, dynamic properties such as self-diffusion and shear viscosity also change depending on the pressure. While self-diffusion decreases abnormally up to the critical pressure value, it exhibits a linear relationship with the pressure after this critical value. On the other hand, shear viscosity increases linearly with the pressure up to the critical pressure value, but it exhibits an abnormal increase after this critical value.

Funding: No funding support has been received from any institution or person

Acknowledgments: We would like to thank Trakya University Rectorate for giving permission and contributing to present this study as a paper.

REFERENCE

[1] W.W. Anderson, T.J. Ahrens, An equation of state for liquid iron and implications for the Earth's core, J. Geophys. Res. Solid Earth 99 (1994) 4273–4284.

[2] D.P. Dobson, Self-diffusion in liquid Fe at high pressure, Phys. Earth Planet. Inter. 130 (2002) 271–284.

[3] L.S. Dubrovinsky, S.K. Saxena, F. Tutti, S. Rekhi, T. LeBehan, In Situ X-Ray Study of Thermal Expansion and Phase Transition of Iron at Multimegabar Pressure, Phys. Rev. Lett. 84 (2000) 1720–1723.

[4] C. Sanloup, F. Guyot, P. Gillet, G. Fiquet, R.J. Hemley, M. Mezouar, I. Martinez, Structural changes in liquid Fe at high pressures and high temperatures from Synchrotron X-ray Diffraction, Europhys. Lett. 52 (2000) 151–157.

[5] M.D. Rutter, R.A. Secco, H. Liu, T. Uchida, M.L. Rivers, S.R. Sutton, Y. Wang, Viscosity of liquid Fe at high pressure, Phys. Rev. B 66 (2002) 060102.

[6] C. Sanloup, F. Guyot, P. Gillet, Y. Fei, Physical properties of liquid Fe alloys at high pressure and their bearings on the nature of metallic planetary cores, J. Geophys. Res. Solid Earth 107 (2002) 2272.

[7] S. Hosokawa, M. Inui, K. Matsuda, D. Ishikawa, A.Q.R. Baron, Damping of the collective modes in liquid Fe, Phys. Rev. B 77 (2008) 174203.

[8] M. Inui, K. Maruyama, Y. Kajihara, M. Nakada, Icosahedral ordering in liquid iron studied via x-ray scattering and Monte Carlo simulations, Phys. Rev. B 80 (2009) 180201.

[9] T. Schenk, D. Holland-Moritz, V. Simonet, R. Bellissent, D.M. Herlach, Icosahedral Short-Range Order in Deeply Undercooled Metallic Melts, Phys. Rev. Lett. 89 (2002) 075507.

[10] G. Shen, V.B. Prakapenka, M.L. Rivers, S.R. Sutton, Structure of Liquid Iron at Pressures up to 58 GPa, Phys. Rev. Lett. 92 (2004) 185701.

[11] Y. Kuwayama, G. Morard, Y. Nakajima, K. Hirose, A.Q.R. Baron, S.I. Kawaguchi, T. Tsuchiya, D. Ishikawa, N. Hirao, Y. Ohishi, Equation of State of Liquid Iron under Extreme Conditions, Phys. Rev. Lett. 124 (2020) 165701.

[12] M.J. Gillan, D. Alfè, J. Brodholt, L. Vočadlo, G.D. Price, First-principles modelling of Earth and planetary materials at high pressures and temperatures, Reports Prog. Phys. 69 (2006) 2365–2441.
[13] L.E. González, D.J. González, Structure and Dynamics in Liquid Iron at High Pressure and Temperature. A First Principles Study, J. Geophys. Res. Solid Earth 128 (2023) e2022JB025119.
[14] A.P. Sutton, J. Chen, Long-range Finnis–Sinclair potentials, Philos. Mag. Lett. 61 (1990) 139–146.
[15] A.B. Belonoshko, R. Ahuja, B. Johansson, Quasi– Ab Initio Molecular Dynamic Study of Fe Melting, Phys. Rev. Lett. 84 (2000) 3638–3641.
[16] T. Bryk, A.B. Belonoshko, Collective excitations in molten iron above the melting point: A generalized collective-mode analysis of simulations with embedded-atom potentials, Phys. Rev. B 86 (2012) 024202.
[17] A.B. Belonoshko, S. Arapan, A. Rosengren, An ab initio molecular dynamics study of iron phases at high pressure and temperature, J. Phys. Condens. Matter 23 (2011) 485402.
[18] Y.D. Fomin, V.N. Ryzhov, V. V Brazhkin, Properties of liquid iron along the melting line up to Earth-core pressures, J. Phys. Condens. Matter 25 (2013) 285104.
[19] L. Vočadlo, G.A. de Wijs, G. Kresse, M. Gillan, G.D. Price, First principles calculations on crystalline and liquid iron at Earth's core conditions, Faraday Discuss. 106 (1997) 205–218.
[20] D. Alfè, G. Kresse, M.J. Gillan, Structure and dynamics of liquid iron under Earth's core conditions, Phys. Rev. B 61 (2000) 132–142.
[21] G.A. de Wijs, G. Kresse, L. Vočadlo, D. Dobson, D. Alfè, M.J. Gillan, G.D. Price, The viscosity of liquid iron at the physical conditions of the Earth's core, Nature 392 (1998) 805–807.
[22] F. Cleri, V. Rosato, Tight-binding potentials for transition metals and alloys, Phys. Rev. B 48 (1993) 22–33.
[23] M.A. Karolewski, Tight-binding potentials for sputtering simulations with FCC and BCC metals, Radiat. Eff. Defects Solids 153 (2001) 239–255.
[24] W. Smith, T.R. Forester, DL_POLY_2.0: A general-purpose parallel molecular dynamics simulation package, J. Mol. Graph. 14 (1996) 136–141.
[25] M. Celtek, S. Sengul, U. Domekeli, V. Guder, Molecular dynamics simulations of glass formation, structural evolution and diffusivity of the Pd-Si alloys during the rapid solidification process, J. Mol. Liq. 372 (2023) 121163.
[26] Y. Waseda, "The Structure of Non-Crystalline Materials, Liquid and Amorphous Solid, McGraw-Hill, New York., 1980.
[27] S. S. Dalgic, U. Domekeli, Melting properties of tin nanoparticles by molecular dynamics simulation, J. Optoelectron. Adv. Mater. 11 (2009) 2126–2132.